

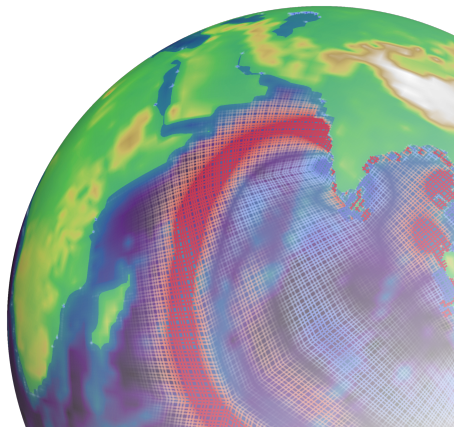
Large-Scale Tsunami Simulations using the Discontinuous Galerkin Method

Boris Bonev ¹ Francis X. Giraldo ² Jan S. Hesthaven ¹

¹Ecole Polytechnique Fédérale de Lausanne

²Naval Postgraduate School, Monterey

27th Biennial Conference on Numerical Analysis
Glasgow, June 27, 2017



- ① Physical Model & Numerical Scheme
- ② Well-Balanced Property
- ③ Wetting/Drying
- ④ Conclusion

Section 1

Physical Model & Numerical Scheme

1D Shallow Water Equations

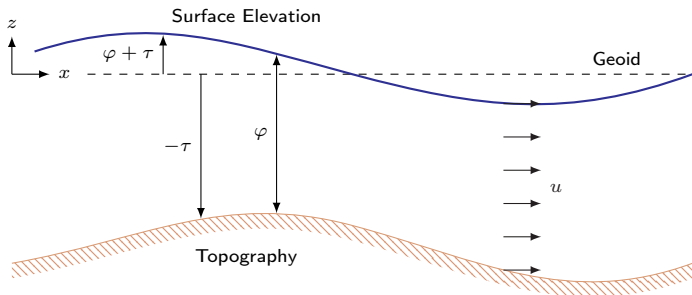


Figure: Notation of the 1D Shallow Water Equations

The Shallow Water Equations in one dimension:

$$\frac{\partial}{\partial t} \varphi + \frac{\partial}{\partial x} (\varphi u) = 0 \quad (1)$$

$$\frac{\partial}{\partial t} (\varphi u) + \frac{\partial}{\partial x} \left(\varphi u^2 + \frac{1}{2} \varphi^2 \right) = - \frac{\partial}{\partial x} \tau \quad (2)$$

Spherical Shallow Water Equations

Scheme based on¹. We use *cartesian coordinates* and therefore have a 4D state vector

$$\mathbf{q} = [\varphi \quad \varphi u \quad \varphi v \quad \varphi w]^T. \quad (3)$$

The Spherical Shallow Water equations in conservation form are then

$$\frac{\partial \mathbf{q}}{\partial t} + \nabla \cdot \mathbf{F}(\mathbf{q}) = \mathbf{S}(\mathbf{x}, \mathbf{q}), \quad (4)$$

where the divergence acts on the unit vectors $\hat{\mathbf{i}}, \hat{\mathbf{j}}, \hat{\mathbf{k}}$ of the flux

$$\mathbf{F}(\mathbf{q}) = \begin{bmatrix} \varphi u \\ \varphi u^2 + \frac{1}{2}\varphi^2 \\ \varphi uv \\ \varphi uw \end{bmatrix} \hat{\mathbf{i}} + \begin{bmatrix} \varphi v \\ \varphi uv \\ \varphi v^2 + \frac{1}{2}\varphi^2 \\ \varphi vw \end{bmatrix} \hat{\mathbf{j}} + \begin{bmatrix} \varphi w \\ \varphi uw \\ \varphi vw \\ \varphi w^2 + \frac{1}{2}\varphi^2 \end{bmatrix} \hat{\mathbf{k}}. \quad (5)$$

The source term incorporates Coriolis force, bottom topography and the Lagrangian forcing term μ :

$$\mathbf{S}(\mathbf{x}, \mathbf{q}) = -\frac{2\Omega z \varphi}{R^2} \mathbf{x} \times \mathbf{u} - \varphi \nabla \tau + \mu \mathbf{x}, \quad (6)$$

where \mathbf{x} is the coordinate (radius) vector.

¹F X Giraldo, Jan S Hesthaven, and T Warburton. "Nodal High-Order Discontinuous Galerkin Methods for the Spherical Shallow Water Equations". In: *Journal of Computational Physics* 181.2 (Sept. 2002), pp. 499–525.

Representation of the solution

The exact solution is represented by piecewise polynomials of degree N^2 in each of the cells D^k :

$$\mathbf{q}(\mathbf{x}, t) \approx \mathbf{q}_N(\mathbf{x}, t) = \bigoplus_{k=1}^K \mathbf{q}_N^k(\mathbf{x}, t). \quad (7)$$

Using the $(N + 1)^2$ Legendre-Gauss-Lobatto quadrature points on the reference element $I = [-1, 1] \times [-1, 1]$ we define the $(N + 1)^2$ Lagrange-polynomials $L_j(\xi)$. Using these polynomials, the solution is represented by

$$\mathbf{q}_N^k(\mathbf{x}) = \sum_{j=1}^{(N+1)^2} \mathbf{q}_N^k(\mathbf{x}_i) L_j(\xi(\mathbf{x})). \quad (8)$$

in each of the cells D^k .

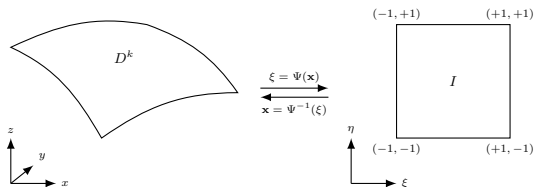


Figure: Transformation into the reference element.

Discontinuous Galerkin formulation

We use the common weak form of the Discontinuous Galerkin method, which is based on the variational formulation of the problem:

Weak Form/Green's Form

$$\forall k, i : \int_{D^k} \left(\frac{\partial \mathbf{q}_N}{\partial t} - \mathbf{F}_N \cdot \nabla - \mathbf{S}_N \right) L_i(\mathbf{x}) d\mathbf{x} = - \oint_{\delta D^k} \hat{\mathbf{n}} \cdot \mathbf{F}_N^* L_i(\mathbf{x}) d\mathbf{x} \quad (9)$$

An additional integration by parts yields the less common strong form:

Strong Form/Divergence Form

$$\forall k, i : \int_{D^k} \left(\frac{\partial \mathbf{q}_N}{\partial t} + \nabla \cdot \mathbf{F}_N - \mathbf{S}_N \right) L_i(\mathbf{x}) d\mathbf{x} = \oint_{\delta D^k} \hat{\mathbf{n}} \cdot (\mathbf{F}_N - \mathbf{F}_N^*) L_i(\mathbf{x}) d\mathbf{x} \quad (10)$$

where \mathbf{F}_N , \mathbf{S}_N are the numerical representations of the flux and source terms and $\mathbf{F}_N^*(\mathbf{q}^+, \mathbf{q}^-)$ is a suitable numerical flux.

We introduce shorthand operators for the gaussian quadrature:

$$\begin{aligned} \mathcal{N} \int_D f(\mathbf{x}) d\mathbf{x} &:= \sum_{i,j=1}^N f(\mathbf{x}(\xi_i, \eta_j)) J(\xi_i, \eta_j) \omega_i^\xi \omega_j^\eta \\ &\approx \int_D f(\mathbf{x}) d\mathbf{x} = \int_I f(\mathbf{x}(\xi)) J(\xi) d\xi \end{aligned} \quad (11)$$

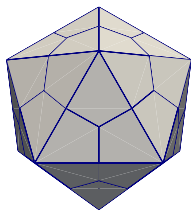
Surface Integrals:

$$\begin{aligned} \mathcal{N} \oint_{\delta D} f(\mathbf{x}) d\mathbf{x} &:= \sum_{i=1}^N f(\mathbf{x}(\xi_i, -1)) J(\xi_i, -1) \omega_i^\xi + \sum_{j=1}^N f(\mathbf{x}(1, \eta_j)) J(1, \eta_j) \omega_j^\eta \\ &\quad + \sum_{i=1}^N f(\mathbf{x}(\xi_i, 1)) J(\xi_i, 1) \omega_i^\xi + \sum_{j=1}^N f(\mathbf{x}(-1, \eta_j)) J(-1, \eta_j) \omega_j^\eta \\ &\approx \oint_{\delta D} f(\mathbf{x}) d\mathbf{x} = \oint_{\delta I} f(\mathbf{x}(\xi)) J(\xi) d\xi \end{aligned} \quad (12)$$

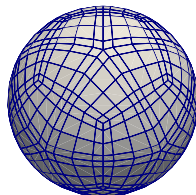
By replacing the integrals and solutions with their numerical counterparts, we retrieve the discontinuous Galerkin scheme.

Icosahedral Grid

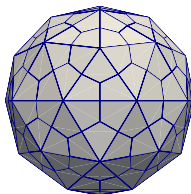
The quadrilateral grids are generated on an initial icosahedron or cube through subdivision and projection.



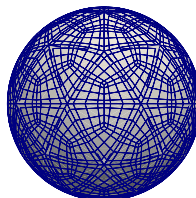
(a) $n_{ref} = 0$



(b) $n_{el} = 6$



(c) $n_{ref} = 1$



(d) $n_{el} = 6$

Section 2

Well-Balanced Property

Well-Balanced Property

Geophysical Systems often have steady-state solutions $\bar{\mathbf{q}}$ such that

$$\frac{\partial \bar{\mathbf{q}}}{\partial t} = 0 \Leftrightarrow \nabla \cdot \mathbf{F}(\bar{\mathbf{q}}) = \mathbf{S}(\mathbf{x}, \bar{\mathbf{q}}). \quad (13)$$

We are mostly interested in the so-called 'water at rest' solution, which is given as

$$\varphi(\mathbf{x}, t) = \varphi_0 - \tau(\mathbf{x}), \quad (14)$$

$$\mathbf{u}(\mathbf{x}, t) = \mathbf{0}. \quad (15)$$

Most of the relevant scenarios involve solutions are (initially) merely a perturbation of this solution. Thus, a common requirement is the well-balanced property:

Well-Balanced Property

A scheme is called well-balanced, if the truncation error disappears for the numerical representation of the steady-state solution $\bar{\mathbf{q}}_N$:

$$\text{RHS}(\bar{\mathbf{q}}_N, \mathbf{x}, t) = 0. \quad (16)$$

Is the Weak Form well-balanced?

We represent the bottom topography with τ_N , which is in the same polynomial space as \mathbf{q}_N . In this case

$$\bar{\mathbf{q}}_N = \begin{bmatrix} \varphi_0 - \tau_N \\ \mathbf{0} \end{bmatrix} \quad (17)$$

satisfies $\nabla \cdot \mathbf{F}(\bar{\mathbf{q}}_N) = \mathbf{S}(\bar{\mathbf{q}}_N, \mathbf{x})$. We require the bottom topography to be continuous and insert this into the righthand-side of the weak form:

$$\begin{aligned} \text{RHS}(\bar{\mathbf{q}}_N, \mathbf{x}) &= \mathcal{N} \int_D \mathbf{F}_N(\bar{\mathbf{q}}_N) \cdot \nabla L_i(\mathbf{x}) \, d\mathbf{x} - \mathcal{N} \int_D \mathbf{S}_N(\bar{\mathbf{q}}_N, \mathbf{x}) L_i(\mathbf{x}) \, d\mathbf{x} \\ &\quad + \mathcal{N} \oint_{\delta D} \hat{\mathbf{n}} \cdot \mathbf{F}_N(\bar{\mathbf{q}}_N) L_i(\mathbf{x}) \, d\mathbf{x} \end{aligned} \quad (18)$$

Remark

In general, for the *weak form*, we can only guarantee the well-balanced property if numerical integration is exact! Due to the rational Jacobian, this is not the case here.

(wellbalancing.mp4)

Strong Form

If we proceed similarly in the case of the *strong form* we find that

$$\begin{aligned} \text{RHS}(\bar{\mathbf{q}}_N, \mathbf{x}) &= \mathcal{N} \int_D (\nabla \cdot \mathbf{F}_N(\bar{\mathbf{q}}_N) - \mathbf{S}_N(\mathbf{x}, \bar{\mathbf{q}}_N)) L_i(\mathbf{x}) d\mathbf{x} \\ &\quad - \mathcal{N} \oint_{\delta D} \hat{\mathbf{n}} \cdot (\mathbf{F}_N(\bar{\mathbf{q}}_N) - \mathbf{F}_N^*(\bar{\mathbf{q}}_N^+, \bar{\mathbf{q}}_N^-)) L_i(\mathbf{x}) d\mathbf{x} \\ &= \mathcal{N} \int_D 0 L_i(\mathbf{x}) d\mathbf{x} - \mathcal{N} \oint_{\delta D} \hat{\mathbf{n}} \cdot \mathbf{0} L_i(\mathbf{x}) d\mathbf{x} = 0. \end{aligned} \quad (19)$$

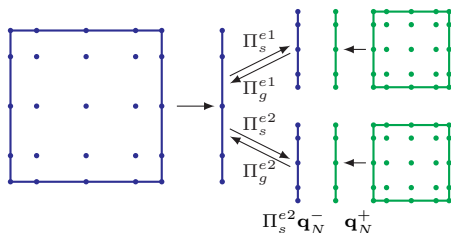
Remark

Each of the integrands becomes point-wise zero, which means that the strong form is well-balanced by construction. This does not require exact numerical integration and generalizes for all continuous steady-state solutions.

(floodedwb.mp4)

well-balanced Adaptive Mesh Refinement

We use non-conforming AMR as presented in². As volume-integrals vanish in the strong form, the well-balanced property carries over nicely to AMR.



well-balanced AMR

Evaluate $\hat{\mathbf{n}} \cdot (\mathbf{F} - \mathbf{F}^*)$ directly on the children edges and project it back to parent:

$$\begin{aligned} & \frac{1}{2} \Pi_g^{e1} [\hat{\mathbf{n}} \cdot [\mathbf{F}_N(\Pi_s^{e1} \mathbf{q}_N^-) - \mathbf{F}_N^*(\Pi_s^{e1} \mathbf{q}_N^-, \mathbf{q}_N^+)]] \\ & + \frac{1}{2} \Pi_g^{e2} [\hat{\mathbf{n}} \cdot [\mathbf{F}_N(\Pi_s^{e2} \mathbf{q}_N^-) - \mathbf{F}_N^*(\Pi_s^{e2} \mathbf{q}_N^-, \mathbf{q}_N^+)]] \end{aligned} \quad (20)$$

²Michal A Kopera and Francis X Giraldo. "Analysis of adaptive mesh refinement for IMEX discontinuous Galerkin solutions of the compressible Euler equations with application to atmospheric simulations". In: *Journal of Computational Physics* 275 (Oct. 2014), pp. 92–117.

Section 3

Wetting/Drying

Some possibilities to handle the wet/dry interface:

- Grid conforming to the wet/dry interface.
 - + Accurate treatment of the interface.
 - Expensive re-meshing and treatment of boundary conditions required.
- Fixed mesh but dry cells are turned off.
 - + Simple to handle.
 - Sudden inclusion/exclusion of the dry elements breaks conservation.
- Keep a thin layer on drying nodes.
 - + Not very expensive and avoids the sudden inclusion/exclusion.
 - Treatment of artificial pressure gradients due to the dry nodes.

Some of the issues at the wet/dry interface:

- How do we maintain positivity on nearly dry nodes?
- How do we evaluate $\frac{(\varphi u)^2}{\varphi}$ for small φ ?
- How can we keep the well-balanced property at the wet/dry interface?

Preserving Positivity of the Average

Idea: Ensure positivity of the average

$$\bar{\varphi} = \int_{D^k} \varphi(\mathbf{x}) d\mathbf{x} \quad (21)$$

in each cell, then rescale the nodal values in order to be positive³.

CFL-like condition

Assuming exact integration, we can show that under the condition

$$\frac{J^e}{J} \Delta t \alpha \leq \frac{\omega_1}{2} \quad (22)$$

where α is the signal velocity, ω_1 the first weight of the numerical integration and J, J^e are the Jacobians of the volume and edge parametrizations respectively.

If we use a convex combination of Euler forward steps, this property is retained. Strong-stability preserving Runge-Kutta (SSPRK) schemes are such schemes⁴.

³Yulong Xing, Xiangxiong Zhang, and Chi-Wang Shu. "Positivity-preserving high order well-balanced discontinuous Galerkin methods for the shallow water equations". In: *Advances in Water Resources* 33.12 (Dec. 2010), pp. 1476–1493.

⁴Sigal Ketcheson David I Shu Chi-Wang Gottlieb. *Strong Stability Preserving Runge-Kutta and Multistep Time Discretizations*. World Scientific Publishing Co., Dec. 2010.

Positivity Limiter

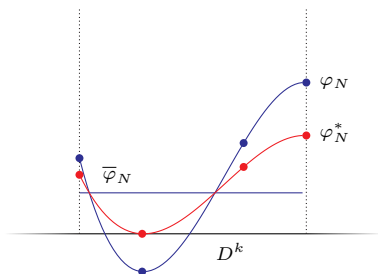


Figure: Application of the positivity limiter

With the average being positive, we can rescale the solution around the average such that the minimal nodal value is ensured to be positive:

$$\theta = \min \left\{ 1, \frac{\bar{\varphi}_N}{\bar{\varphi}_N - m} \right\}, \quad (23)$$

$$m = \min_i \{ \varphi_N(\mathbf{x}_i) \}. \quad (24)$$

The rescaled solution is then:

$$\varphi_N^* = \theta * (\varphi_N - \bar{\varphi}_N) + \bar{\varphi}_N. \quad (25)$$

Well-Balanced Wet/Dry Interface

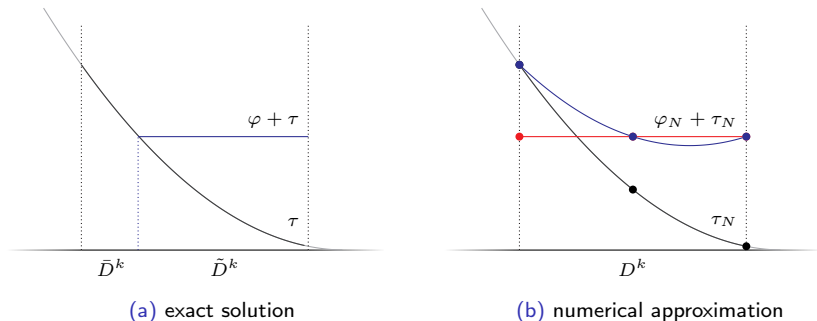


Figure: Interface in the exact and numerical case.

Remark

The positivity limiter ensures positivity, but if we do not allow negative waterheights, we can not ensure $\varphi_N \nabla \varphi_N = -\varphi_N \nabla \tau_N$. Therefore well-balancedness is lost.

(1dwbshore.mp4)

(3dwbshore.mp4)

Well-Balanced Wet/Dry Interface

Solution: Track partly dry cells and set $g = 0$ there⁵.

- + Spurious waves disappear.
- Partly dry cells keep filling up until they are full.
- Conservation of momentum is lost at the interface.

⁵Stefan Vater, Nicole Beisiegel, and Jörn Behrens. "A limiter-based well-balanced discontinuous Galerkin method for shallow-water flows with wetting and drying: One-dimensional case". In: *Advances in Water Resources* 85 (Nov. 2015), pp. 1–13.

(tohoku.mp4)

Figure: 15360 elements with 16 high-order points.

Section 4

Conclusion

Conclusion

- Stable, parallelizable method for the simulation of large-scale Tsunamis.
- The method is adaptive and well-balanced by construction.
- Under the timestep restriction the method is positivity-preserving.
- It handles effects of Earth's curvature natively.
- Boundary conditions are not necessary due to the periodicity of the grid.
- Our results on well-balancedness generalize to curved elements.

Outlook

- Adaptive Mesh Refinement and Wetting/Drying
- Alternative Solutions for Wetting/Drying
- Accuracy of the Wetting/Drying method
- Numerical Experiments & Benchmarks

Thank you for your attention.